International Journal of Analytical, Experimental and Finite Element Analysis
Volume 10, Issue 1, March 2023, pp 1 - 10
https://doi.org/10.26706/ijaefea.1.10.20239252

Finite Element Analysis of Self-Compacted Concrete Filled Steel Tube Columns Exposed to High Temperatures

Waleed Khalid Mohammed, Khamees N. Abdulhaleem, Shwan H. Said, Qais F. Hasan

[1,2] Civil Engineering Department, University of Kirkuk, Kirkuk, Iraq
Email: waleedkhalid@uokirkuk.edu.iq, khamees.civ.str@uokirkuk.edu.iq

[3] Department of Environmental Engineering and Pollution, Technical Engineering College- Kirkuk, Northern Technical University, Iraq.
Email: shwan@ntu.edu.iq

[4] Department of Surveying Engineering, Technical Engineering College- Kirkuk, Northern Technical University, Iraq.
Email: dr.qaishasan@ntu.edu.iq

Corresponding Author: dr.qaishasan@ntu.edu.iq

Abstract: To represent the structural behavior of self-compacted concrete filled steel tube composite columns under axial compression loading after high temperatures exposure, a nonlinear three-dimensional finite element analysis model has been achieved to analyze these columns using ANSYS R-15 software. An eight-node solid brick element (Solid65) is used to represent the concrete, while a four-node isoparametric shell element (Shell63) is used to represent the steel tube for the analyzed composite columns. A Newton-Raphson incremental-iterative approach is used to simulate the nonlinear solution technique. The finite element method results indicated that the predicted ultimate loads and axial deformations for the analyzed four column specimens agree well with the experimental results for normal strength and high strength concrete in static loading up to failure, and therefore, it is sufficient to model how these columns behave. The reduction in the analytical ultimate loads compared to the experimental values ranged from 11% and 16%, while the reduction in the total axial deformation values ranged from 3% to 7%. The yield patterns obtained from the analyzed composite columns under axial compressive stress are comparable to the yield patterns determined from the experimental study.

Keywords: self-compacted, composite column, steel tube, finite element, ANSYS.

Article – Peer Reviewed
Received: 1 March 2023
Accepted: 24 March 2023
Published: 31 March 2023

Cite this article: Waleed Khalid Mohammed, Khamees N. Abdulhaleem, Shwan H. Said, Qais F. Hasan, "Finite Element Analysis of Self-Compacted Concrete Filled Steel Tube Columns Exposed to High Temperatures", *International Journal of Analytical, Experimental and Finite Element Analysis*, RAME Publishers, vol. 10, issue 1, pp. 1-10, 2023.
https://doi.org/10.26706/ijaefea.1.10.202309252

1. Introduction

Concrete Filled Steel Tube (CFST) composite columns are widely used in structures due to their excellent attitude, including superior fire resistance compared to plain steel columns, resistance to seismic loads, efficient use of materials, better strength, higher stiffness, larger ductility, and a noticeably shorter construction time. Composite concrete-steel structural elements are frequently used in modern bridge and building construction [1]. When a steel part, such as a steel tube, is enclosed in concrete or when a steel I-section is filled with concrete, a composite member here is produced. In a CFST like this, the high compression concrete strength matches the high-tension steel strength. Concrete that self-compacts (SCC) is fluid and is cast without vibration [2]. This building material is increasingly employed in flat buildings like slabs or industrial floors because of its self-leveling qualities. However, when concrete is uncovered to hot and/or windy circumstances, this form of construction is particularly susceptible to plastic shrinkage cracking [3]. Investigations were made for the behavior of steel tubular SCC filled stub columns and exposed to a protocoled fire at the same time [4]. The temperature distribution, axial deformation, steel's limiting temperature, and fire resistance of the SCC filled steel tubular stub columns were all measured through a series of experiments. A Finite Element Method (F.E.M) analysis model was also suggested and utilized to simulate the columns' fire behavior.

A F.E.M analytical model was used to predict the load versus deformation relationships of CFST stub columns subjected to temperature and axial compression [5]. A CFST stub columns set were tested under a variety of thermal and mechanical loading conditions with high temperatures to ascertain the specimens' residual strength which were heated evenly. The tests are done on specimens exposed to fire according to the ISO-834 standard with no initial loads. These tests were all simulated using this model. This model may reasonably accurately predict the load versus deformation relationships, according on a comparison of the predicted and test findings. The behavior of CFST stub columns was then investigated using the F.E.M analysis model by looking at the confinement stress development and cross-sectional stress distribution at various loading stages, including initial loading stage in addition to heating and cooling stages. After cooling, all of the specimens were loaded until they failed, and the residual stress index was examined in relation to a number of factors. The ultimate strength was found to be marginally lower when temperature and loading were taken into account than it was after being exposed to fire with no initial load. The peak strain that corresponded to the strength at ultimate was much higher.

Investigation is done into an experimental study result that looked at the behavior of columns with SCC-filled steel tube that had been exposed to high temperatures [6]. Twenty-eight composite column specimens were tested in the lab to determine the during heating temperature distribution, the relationship between load and deformation besides the residual strengths of SCC filled columns after being exposed to high temperatures are studied. The purpose of the experiment was to determine how the behavior of the composite columns was affected by a number of different factors, such as temperature exposure, compressive strength of concrete, diameter of steel tube, and wall thickness of steel tube. The test findings demonstrated that when applied temperature increased, the SCC concrete compressive strength and the failure load of composite columns dropped. After being heated to 400 and 600 ^{o}C, the compressive strength of standard SCC reduced by around 39.77 and 64.55%, whereas the compressive strength of high SCC values decreased by 40.86, 74.38, and 89.35% after being heated to 400, 600, and 800 ^{o}C, respectively. After high temperatures exposure, the failure loads of the normal and high strength composite columns reduced by smaller amounts with the largest reduction ratio occurring at 800 ^{o}C.

Many researchers investigated analytical algorithms using F.E.M to analyses for the concrete filled steel tubes [7, 8]. A F.E.M analysis algorithm was performed [9], using commercial software, to evaluate the performance of Concrete-Filled Double-Skin Tube (CFDST) composite columns exposed to post-earthquake fires. This primary objective was to replicate findings from a series of tests that involved firing the identical specimens in a furnace after cyclic lateral loading which was used to subject CFDST columns to various degrees of seismic damage. In the loading sequence, the numerical algorithm followed the experiments closely. The ability of various material models and modeling approaches to replicate experimental findings, including local failure modes such buckling of steel tube, was evaluated based on their ability to replicate experimental findings including local failure modes like steel tube buckling. In order to recreate the fire testing portion of the tests, the results from the subsequent thermal stress analysis were preserved as initial conditions, including residual deformations. The models of CFDST columns were subjected to a sequentially coupled nonlinear thermal stress analysis to examine the impacts of exposure to a typical fire (time-temperature) curve. A reasonable comparison with experimental results was made for both during and after the fire using numerical simulations that used material parameters adapted from European general principles for structural fire design [10, 11].

2. Aim of research

Using a three-dimensional F.E.M analysis model and statically increased loads up to failure, the current study aims to analyze the behavior of SCC-filled steel tube composite columns exposed to high temperatures. The developed F.E.M model, which would be carried out using the ANSYS R-15 software, will be verified and used to simulate the behavior and predict the ultimate load and deflection capacities of four different composite columns within the up-to-failure loading stage due to axial compression loading after theoretically exposure to high temperatures. The obtained analytical results will to be discussed and compared with the experimental results available in literature.

3. Finite element method analysis model

An efficient tool for the analysis of reinforced concrete structures is the nonlinear F.E.M. It represents the real structure as an amalgamation of a limited number of components. It is conceivably a numerical laboratory procedure. The effectiveness and precision of this artificial lab instrument mostly depend on the stiff and accurate modeling of the particular material properties of steel and concrete. The uncracked elastic stage, the crack propagation stage, and the inelastic stage can be used to roughly categorize the reaction of SCC filled steel composite columns. The three main causes of nonlinearity are steel tube yielding, concrete crushing in compression, and inelastic behavior of concrete in compression [12]. All the experimentally tested SCC steel composite columns are examined in the current study using a nonlinear F.E.M analysis to depict the structural behavior of SCC steel composite columns under axial loading. The analysis was completed using the all-inclusive general purpose finite element computer program ANSYS (ANalysis SYStem Release-15) [13].

3.1 Materials modeling

Concrete is a material that exhibits distinct behavior under compression and tension because it is quasi-brittle. Fig. 1 depicts the followed model of the stress-strain relationship for concrete under tension and compression [14].

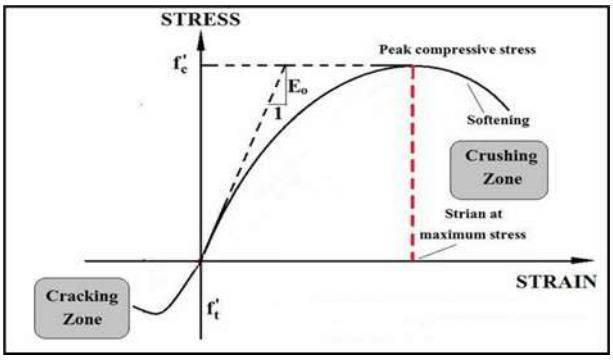

Figure 1. Concrete's typical compressive and tensile stress-strain curves [14].

In concrete any tensile principal stress will cause the material to crack, and all compressive principal stresses will cause crushing [15]. When a material fails under uniaxial, biaxial, or triaxial compression at an integration point, it is assumed to have crushed at that location. Under these circumstances, it is presumable that the material strength at the integration point under consideration has deteriorated to the point where its contribution to an element's stiffness can be disregarded [13]. Concrete fracture under a multiaxial situation of loads is predicted by a failure criterion that shows the limit value [8]. Compared to concrete, steel has a considerably simpler behavior because it is a homogeneous material. For instance, it exhibits the same stress-strain response in both compression and tension. The von Mises yield criterion, which posits that yielding happens when the stress invariant reaches a threshold value, describes the steel tube [15]. To infer a relationship between the plastic strain component and the stress increment, another assumption about material behavior to manage the plastic flow after yielding should be made [16].

3.2 Materials representation

Concrete members are modeled using Solid-65 three-dimensional solid brick elements. This element includes eight nodes, each of which has three degrees of freedom for translation in the x, y, and z axes, as shown in Fig. 2. The element is capable of large deflection geometric nonlinearities, creep nonlinearities, crushing in compression, and cracking in tension. The element can also be used to evaluate reinforced concrete members [13]. The output of the solution is nodal displacements. The stress' normal components in the x, y, and z axes, shear stresses in addition to the main stresses are a few examples of additional element output. The element coordinate system and the element stress directions run in parallel.

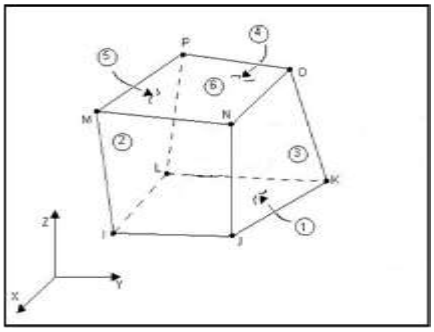

Figure 2. Eight-node brick element (Solid-65) used to model concrete [13].

A bending and membrane-capable isoparamatric shell four-node element from the ANSYS R-15 program with the name (Shell63) [13] has been used for the steel tube representation in the composite columns, as shown in Fig. 3. The element has five degrees of freedom at each node, including the ability to deflect significantly and stiffen under load as well as translations in the nodal x, y, and z directions as well as rotations about the x and y axes of the plane. For application in large deflection (finite rotation) investigations, a constant tangent stiffness matrix option is obtainable [15].

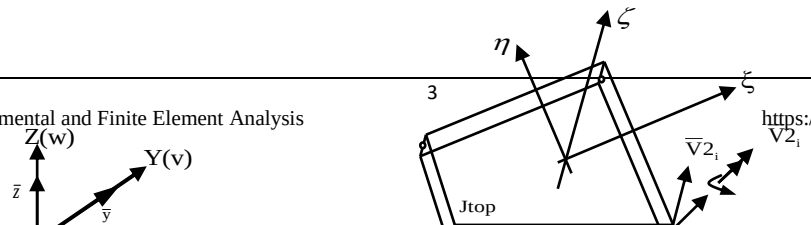

Figure 3. Four-node isoparametric shell element (Shell63) used to model steel tube.

3.3 Numerical integration

Analytical numerical integration, which is required to create the element stiffness matrix, is not feasible. In order to complete the numerical analysis, a different method of numerical integration is needed, therefore, it is crucial to pick an integration method that is accurate and computationally effective. The Gauss Quadrature approach is utilized in the current work since finite element work has demonstrated its usefulness [13]. Brick element's stiffness matrix is expressed using local coordinate axes. The integration rule used in this work is the 8 (2×2×2) points rule, as shown in Fig. 4. Location of the sampling points and the 2×2×2 integration rule weighting factors are shown in Table 1.

Table 1. Integration rule locations of the sampling points and the weighting variables [12, 13].

Sampling Point	Load Coordinates			Weight
	ξ	η	ζ	
1-8	± 0.57734	± 0.57734	± 0.57734	1

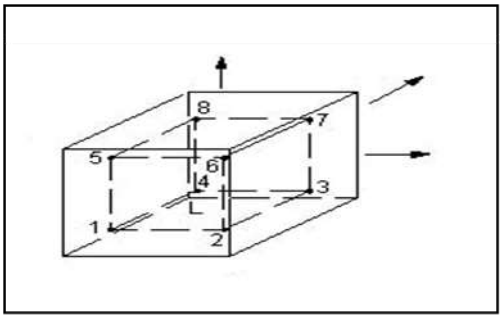

Figure 4. Location of integration points for the 8-node brick element [13].

3.4 Nonlinear solution technique

The whole Newton-Raphson algorithm is integrated with incremental-iterative solution processes in the ANSYS R-15 program that has been put into use. When nonlinear structural problems are discretized using finite elements, a nonlinear algebraic equations set has the form:

$$[K]\{U\} = \{F_a\} \quad \text{..... (1)}$$

where:

$[K]$= matrix of stiffness.

$\{U\}$= nodal displacements vector.

$\{F_a\}$= applied loads vector.

Equation (1) is used to solve for the unknown displacements *{U}* in linear elastic situations. The stiffness matrix *[K]* for a nonlinear system is a function of the unidentified displacements (or their derivatives). Therefore the unknown displacements *{U}* have to be determined precisely before computing equation (1).

3.5 Geometry of SCC filled steel composite columns

Some of SCC filled steel tube columns that have been exposed to high temperatures and experimentally tested in literature [6] are analyzed in the present study. All the tested composite column specimens had an identical height of 500 mm. Composite columns were tested using two groups:

1- Concrete composite columns of 76 mm external diameter with steel wall thicknesses of 1.4 and 1.8 mm, as sketched in Fig. 5a.
2- Concrete composite columns of 101 mm external diameter with steel wall thicknesses of 1.8 and 2.8 mm, as sketched in Fig. 5b.

All these composite columns were loaded axially in compression, and their components via the proposed analytical method are shown in Fig. 6. Material properties and additional material parameters adopted in the F.E.M analysis are shown in Table 2. The followed F.E.M mesh model discretization for a typical column specimen is shown in Fig. 7.

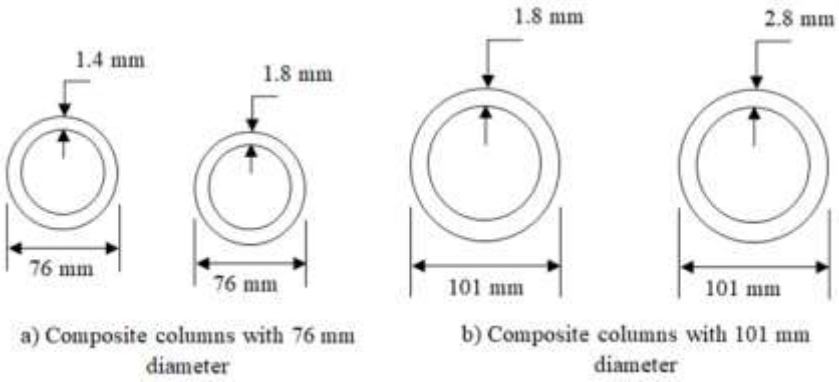

Figure 5. Composite SCC columns used in the analysis [6].

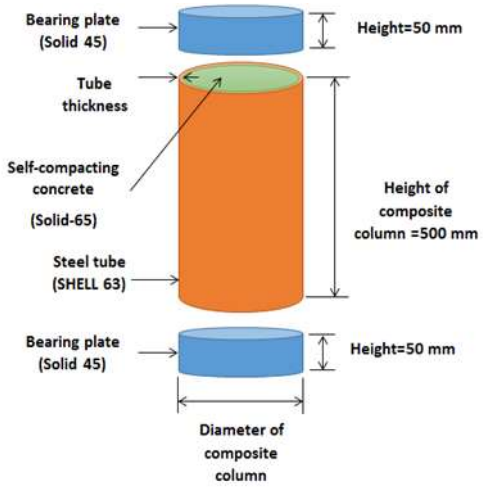

Figure 6. F.E.M components of a typical SCC composite column specimen.

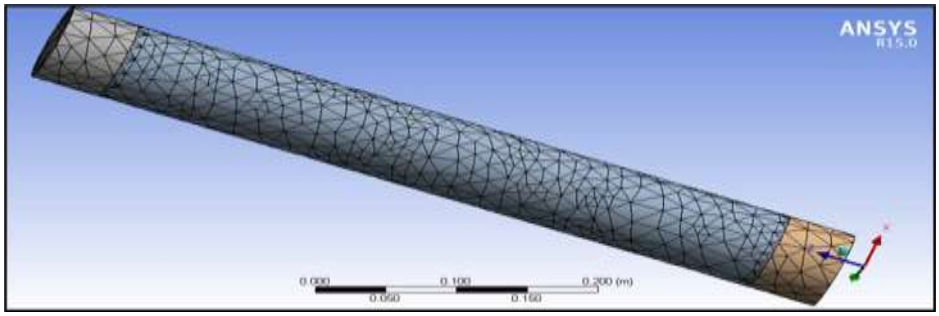

Figure 7. F.E.M mesh discretization used for a typical SCC composite column.

Table 2. Material properties and parameters used for the composite column specimens.

Temperature (°C)	f'c (MPa)		Ec* (MPa)		ν_c		fy (MPa)	Es (MPa)	ν_s
	NS	HS	NS	HS	NS	HS			
25	44	49.8	31176	33167	0.2	0.2	340	200000	0.284
400	26.5	29.45	24194	25505	0.2	0.2	300	168000	0.299
600	15.6	12.76	18563	16788	0.2	0.2	260	116000	0.308
800	9.7	5.3	14638	10820	0.2	0.2	230	66000	0.316

* $E_c = 4700\sqrt{f_c'}$

3.6 Analysis procedure for SCC filled steel composite columns

An SCC filled steel composite columns that were exposed to axial compressive loading serves as the element model for this investigation. The static analysis type here is applied for axial loading up-to-failure. The procedure is based on static minor displacements for the specific instance that is being looked at in this work. The substeps were configured to display the load increments that were used for nonlinear analysis are shown in Table 3. The commands used to control the solution and outputs are shown in Table 4. The commands used for the nonlinear algorithm and convergence criteria are shown in Table 5.

Table 3. Control commands for nonlinear analysis.

Analysis options	Small displacement
Calculate prestress effects	No
Time at end of load step	1000
Automatic time stepping	On
Number of sub step	25
Maximum number of sub step	25
Write items to results file	All solution items
Frequency	Write every sub step

Table 4. Commands for output managing.

Equation solver	Sparse
Number of restart file	1
Frequency	Write every sub step

Table 5. Nonlinear algorithm and convergence criteria parameters.

Line search	On
DOF solution predictor	Prog. chooser
Maximum number of iteration	100
Cutback control	Cutback according to predicted number of iteration
Equivalent plastic strain	0.15
Explicit creep ratio	0.1
Implicit creep ratio	0
Incremental displacement	10,000,000
Set convergence criteria	
Label	U
Reference value	Calculated
Tolerance	0.05
Norm	Infinite norm
Minimum reference	Not applicable

4. Results and discussion

4.1 Load-axial deformation relationship

The top face of the SCC filled steel composite column specimens was used to measure total axial deformations. Fig. 8 illustrates the deflected shape at ultimate load of the normal strength concrete composite column $CNt_1D_1T_1$ according to F.E.M analysis findings caused by an axial force at 25 °C. This column has wall thickness of 1.4 mm and outer diameter of 76 mm. The deflected shape at ultimate load of the high strength concrete composite column $CHt_2D_2T_2$ according to the F.E.M analysis at 400 °C is shown in Fig. 9. This column has wall thickness of 1.8 mm and outer diameter of 101

mm. A comparison between analytical and experimental load-axial deformation curves for normal and high strength concrete for four different SCC filled steel tube column specimens are shown through Table 6 and Figs. 10-13.

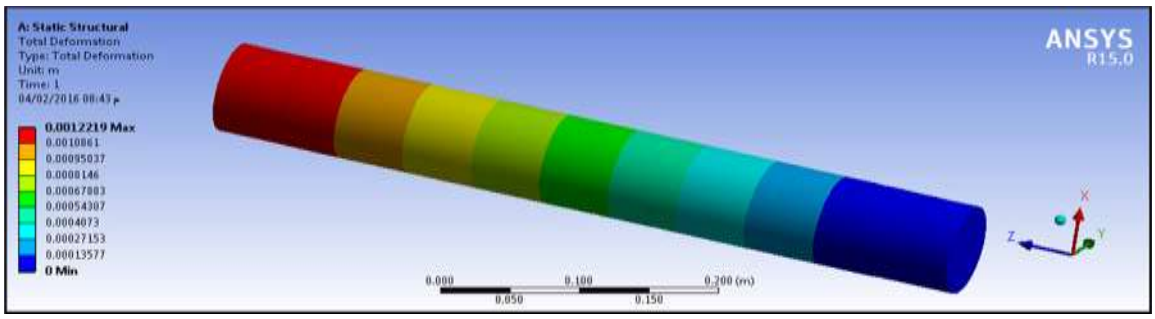

Figure 8. Variation in displacement UZ along column $CNt_1D_1T_1$ at ultimate load.

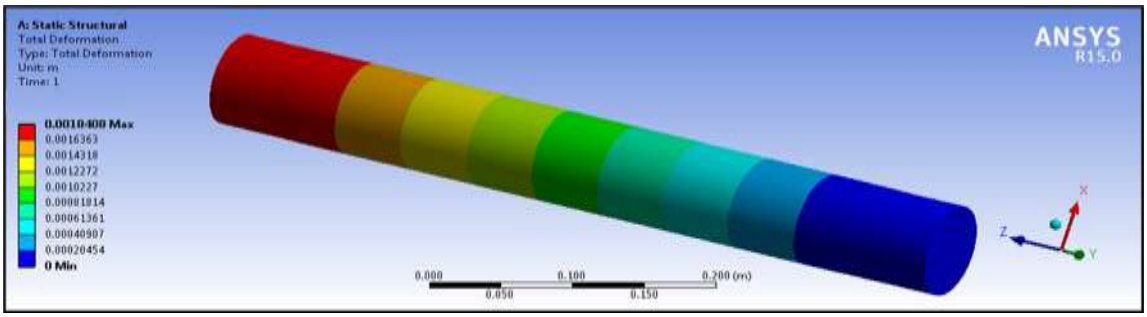

Figure 9. Variation in displacement UZ along column $CHt_2D_2T_2$ at ultimate load.

Table 6. Analytical and experimental results comparison.

Specimen No.	Experimental results [6]				Analytical results		Reduction in ultimate axial load (%)	Reduction in ultimate axial deform. (%)
	f'c (Mpa)	Temp. at test (°C)	Ultimate axial load (kN)	Ultimate axial deform. (mm)	Ultimate axial load (kN)	Ultimate axial deform. (mm)		
CNt1D1T1	44.0	25	474.46	10.51	417.18	10.22	12	3
CNt2D1T1	44.0	25	436.99	11.08	370.42	10.56	15	5
CHt1D1T1	49.8	25	520.45	12.60	461.30	12.12	11	4
CHt2D2T2	29.5	400	736.49	16.61	615.41	15.38	16	7

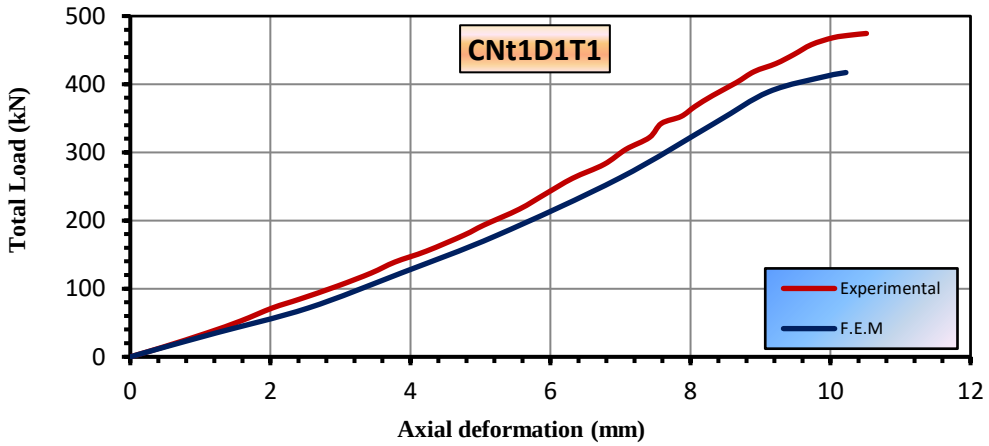

Figure 10. Analytical and experimental load-axial deformation curves for column $CNt_1D_1T_1$.

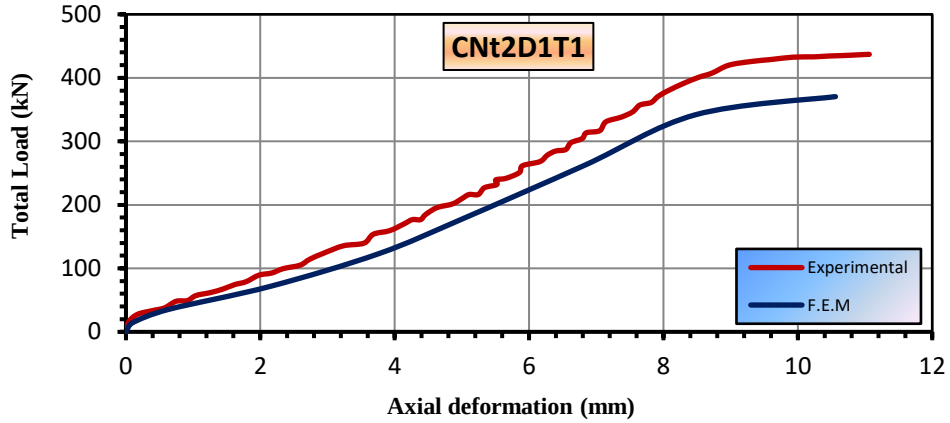

Figure 11. Analytical and experimental load-axial deformation curves for column $CNt_2D_1T_1$.

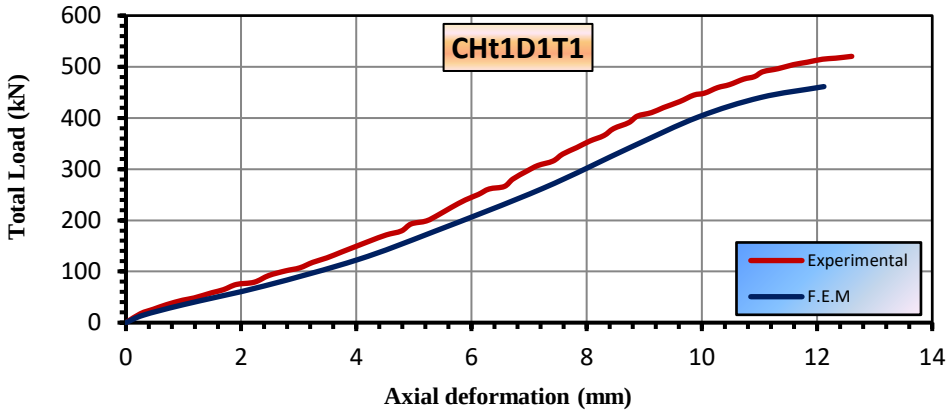

Figure 12. Analytical and experimental load-axial deformation curves for column $CHt_1D_1T_1$.

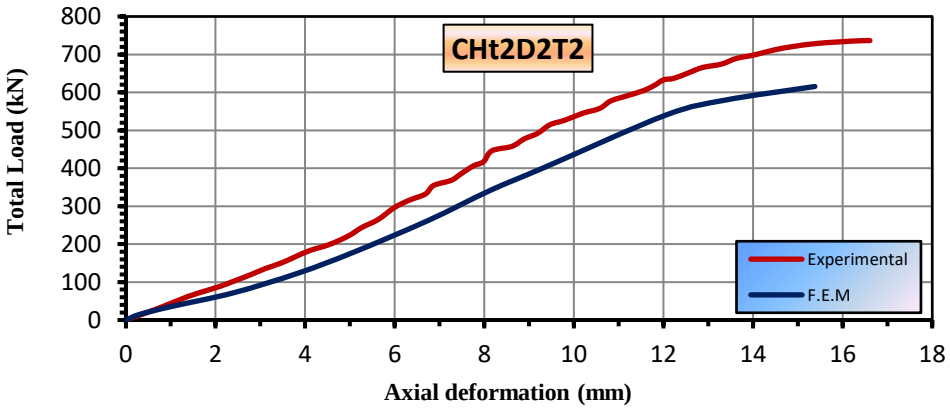

Figure 13. Analytical and experimental load-axial deformation curves for column $CHt_2D_2T_2$.

In general, the computed analytical ultimate axial loads are just a little bit lesser than the recorded experimental values for all the analyzed four column specimens. The ultimate load for the normal strength concrete of 1.4 mm steel wall thickness composite column $CNt_1D_1T_1$ is 12% less than the experimental value, while the analytical ultimate axial deformation is reduced by 3% compared to the recorded experimental result, as shown in Table 6 and Fig. 10. This means that the adopted F.E.M model result agrees well with the experimental result, in spite of the fact that it gives a slightly conservative response. The load-axial deformation curves, both analytical and experimental, are shown and compared in Fig. 11 for the 1.8 mm steel wall thickness composite column $CNt_2D_1T_1$ with the same other specifications as for $CNt_1D_1T_1$ column. The F.E.M analysis ultimate load is 15% lesser than the experimental value, while the axial deformation is reduced by 5% compared to the experimental value. The predicted ultimate load for the high strength concrete composite column $CHt_1D_1T_1$ with 76 mm outer diameter and 1.4 mm wall thickness is less than the experimental

value by 11%, while for the high strength concrete composite column $CHt_2D_2T_2$, with 101 mm outer diameter and 1.8 mm wall thickness, the predicted ultimate load is 16% lower than the experimental value, and this represents the maximum calculated difference percentage between the analytical and experimental ultimate loads. The ultimate analytically predicted axial deformations are reduced by 4% and 7% for these columns, respectively, when compared with the experimental result. This means that the analytical results perform with good agreement with the experimental results, but with a relatively conservative response due to the conservative concrete model followed in F.E.M analysis procedure. Moreover, the stiffer response of the experimental results may be attributed to the behavior of concrete inside the steel tube which may exhibit a type of confinement which is not being considered in the F.E.M analysis.

4.2 Yielding stress pattern

The yielding stress pattern at each loading analysis can be displayed in the ANSYS computer program, as demonstrated in Figs. 14-16, for normal strength composite columns $CNt_1D_1T_1$, $CNt_2D_1T_2$, and $CNt_3D_2T_3$, at 25 ºC, 400 ºC, and 600 ºC, respectively. The yielding stress patterns derived from the F.E.M analysis and failure modes of the experimental composite columns are in good agreement.

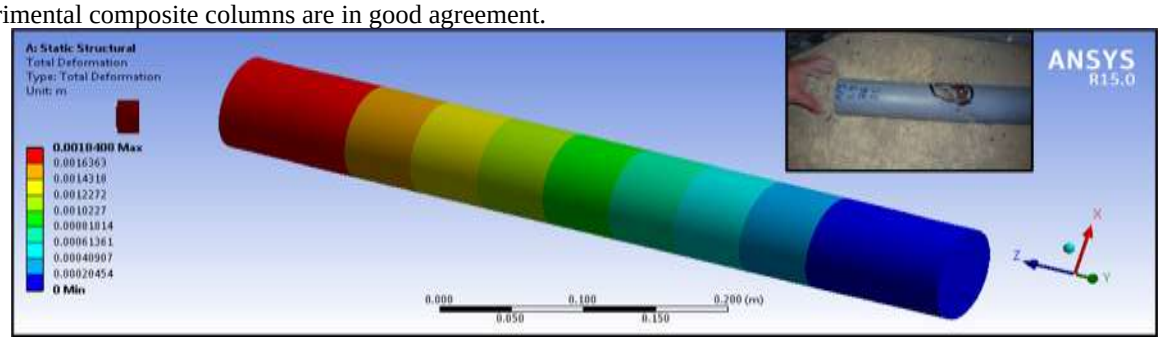

Figure 14. Analytical and experimental stress pattern of column $CNt_1D_1T_1$.

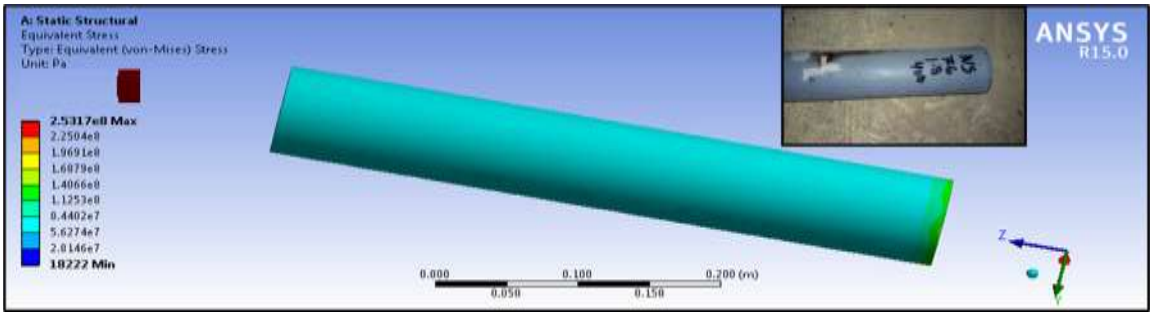

Figure 15. Analytical and experimental stress pattern of column $CNt_2D_1T_2$.

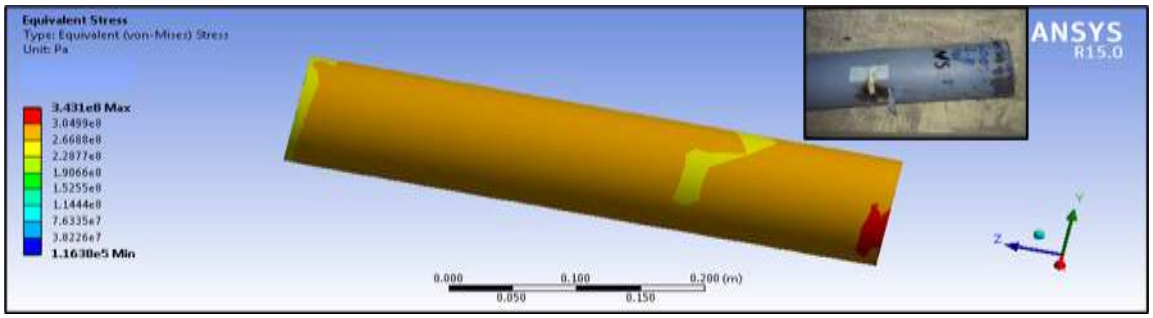

Figure 16. Analytical and experimental stress pattern of column $CNt_3D_2T_3$.

5. Conclusions

The current study's numerical F.E.M. analysis results led to the following conclusions:

1. The F.E.M analytical model utilized in this study is sufficient to simulate the behavior of SCC filled steel composite columns under axial compressive force. For both normal and high strength SCC composite columns, and at normal and elevated temperatures. The predicted behavior and ultimate load by F.E.M. analysis are in good agreement with the experimental results. The numerical ultimate load can vary by up to 16% from the experimental value.

2. A comparison between the analytical and experimental behaviors shows a slightly stiffer response for the experimental results, which may be attributed to the behavior of concrete inside the steel tube which exhibits a type of confinement which is not being considered in the F.E.M analysis.
3. The load-axial deformation curves under axial compressive loading depict the behavior of the analytically studied composite columns and exhibit good agreement with the corresponding experimental data. The composite columns that have undergone numerical analysis, however, have a slightly softer response in both the linear and nonlinear regimes, with 7% maximum difference in ultimate axial deformation when compared with the experimental result.
4. Under axial compressive loading, the yield patterns derived from the studied composite columns are comparable to the yield patterns concluded from the experimental study.

References

[1] Oehlers, D. J., and Bradford, M. A., Elementary Behavior of Composite Steel and Concrete Structural Members, Butterworth Heinemann, 1999, London. https://doi.org/10.1201/b12849

[2] Turcry, P., and Loukili, A., "Evaluation of Plastic Shrinkage Cracking of Self-Consolidating Concrete", ACI Material Journal, Vol. 103, No. 4, July-August, 2006, pp. 272-279. https://doi.org/10.14359/16611

[3] Ameen, Y. M., "Reinforced Self-Compacted Concrete Filled Steel Tube Columns", M.Sc thesis, Graduate School of Natural and Applied Sciences, University of Gaziantep, Turkey, 2018, 93 pages.

[4] Lua H., Zhaoa X., and Hanb L., "Fire Behavior of High Strength Self-Consolidating Concrete Filled Steel Tubular Stub Columns", Journal of Constructional Steel Research, Elsevier Science Publishers, Vol. 65, 2009, pp. 1995-2010. https://doi.org/10.1016/j.jcsr.2009.06.013

[5] Song T., Han L., and Yu H., "Concrete Filled Steel Tube Stub Columns under Combined Temperature and Loading", Journal of Constructional Steel Research, Elsevier Science Publishers, Vol. 66, 2010, pp. 369-384. https://doi.org/10.1016/j.jcsr.2009.10.010

[6] Fahmi H. M., Jweeg M. J., and Khalid O., "Behavior of Self-Consolidating Concrete Filled Steel Tube Columns Subjected to High Temperatures", Proceeding of 15th Scientific Conference, Al-Mansour University College, Baghdad, Iraq, 23-24 April 2016.

[7] Sarir, P., Jiang, H., Asteris P. G., Formisano, A., and Armaghani, D. J., "Iterative Finite Element Analysis of Concrete-Filled Steel Tube Columns Subjected to Axial Compression", Buildings, Vol. 12, No. 12, 2022. https://doi.org/10.3390/buildings12122071

[8] Qasim O. A., "Numerical investigation analysis of variables effect on composite concrete filled steel tube columns", AIP Conference Proceedings, Vol. 2213, No. 1, 2020. https://doi.org/10.1063/5.0000207

[9] Imani, R., Mosqueda, G., and Bruneau, M., "Finite Element Simulation of Concrete-Filled Double-Skin Tube Columns Subjected to Post earthquake Fires", Journal of Structural Engineering, Vol. 141, No. 12, December 2015. https://doi.org/10.1061/(ASCE)ST.1943-541X.0001301

[10] [Hai, T. S., Lin, H. H., and Hong, H. Y., "Concrete filled steel tube stub columns under combined temperature and loading", Journal of Constructional Steel Research, Vol. 66, No. 3, 2009, pp. 369-384. https://doi.org/10.1016/j.jcsr.2009.10.010

[11] Xu, L., Pan, J., Yang, X., "Mechanical performance of self-stressing CFST columns under uniaxial compression", Journal of Building Engineering, Vol. 44, 2021. https://doi.org/10.1016/j.jobe.2021.103366

[12] Dawe, D. J., Matrix and Finite Element Displacement Analysis of Structures, Clarendon Press, Oxford, U. K., 1984, 565 pp. https://doi.org/10.1137/1029025

[13] ANSYS, "ANSYS Help", Release-15, Copyright 2015.

[14] Bangash M. Y. H., "Concrete and Concrete Structures: Numerical Modeling and Applications", Elsevier Science Publishers, Ltd., England, 1989.

[15] Chapman, J. C., Dowling, P. J., Lim, P. T. K., and Billington, C. J., "The Structural Behavior of Steel and Concrete Box Girder Bridges", Journal of Structural Engineering, Vol. 49, No. 3, 1971, pp. 111-120.

[16] Han, L., and Lin, X., "Tests on Cyclic Behavior of Concrete-Filled Hollow Structural Steel Columns after Exposure to the ISO-834 Standard Fire", Journal of Structural Engineering, ASCE, Vol. 130, No. 11, November 2004, pp.1807-1819. https://doi.org/10.1061/(ASCE)0733-9445(2004)130:11(1807)